



## Biosorption of toxic congo red dye from aqueous solution by eco-friendly biosorbent *Saccharum bengalense*: kinetics and thermodynamics

Muhammad Imran Din<sup>a,b</sup>, Zaib Hussain<sup>b,\*</sup>, Muhammad Latif Mirza<sup>a</sup>  
Muhammad Makshoof Athar<sup>b</sup>, Asadullah Madni<sup>c</sup>, Saeed Ahmad<sup>c</sup>

<sup>a</sup>Department of Chemistry, The Islamia University of Bahawalpur, Bahawalpur 63100, Pakistan

<sup>b</sup>Institute of Chemistry, University of Punjab, Lahore 54590, Pakistan

Tel. +92 334 439 6809; Fax: +92 42 9923 1269; email: drzh1972@hotmail.com

<sup>c</sup>Department of Pharmacy, The Islamia University of Bahawalpur, Bahawalpur 63100, Pakistan

Received 26 November 2011; Accepted 10 December 2012

### ABSTRACT

In the present study, *Saccharum bengalense* (SB), a potential biosorbent, was investigated for the removal of toxic Congo red (CR) dye. The effect of various operating variables, viz. adsorbent dosage, pH, contact time, and temperature on the removal of dye has been studied. Almost 94% removal of dye is possible after 50 min at pH 2.0 under batch test conditions. It was found that a pseudo-second-order mechanism was predominant and the overall rate of the dye adsorption process appears to be controlled by more than one step. The intra-particle diffusion model was applied to investigate the rate determining step. Langmuir, Freundlich, and Dubinin–Radushkevich adsorption isotherm models were applied to describe the biosorption isotherm. The biosorption data were better represented by the Langmuir model and the biosorption capacity ( $q_{\max}$ ) of SB for CR was achieved at 125 mg/g. Thermodynamic parameters such as standard free energy change ( $\Delta G^\circ$ ), standard enthalpy change ( $\Delta H^\circ$ ), and standard entropy change ( $\Delta S^\circ$ ) were calculated and revealed the spontaneous, endothermic, and feasible nature of the adsorption process. Biomass derived from the pulp of SB was evaluated as an effective biosorbent for removal of CR dye.

*Keywords:* Biosorbent; *Saccharum bengalense*; Congo red; Kinetics

### 1. Introduction

Dyes are important water pollutants which are generally present in the effluents of textile, paper, and dye manufacturing industries. The colored dye effluents are generally considered to be highly toxic to the aquatic system. Some dyes are reported to cause skin

irritation, dermatitis, allergy, and cancer in humans [1,2]. Thus, the elimination of dyes from effluents before mixing with unpolluted natural water bodies is important. Congo red (CR) dye, commonly used in silk clothing manufacture, is difficult to dispose off in an environmentally benevolent way. The dye is known to metabolize to benzidine, a known human carcinogen. Exposure to the dye has been known to

\*Corresponding author.

cause an allergic reaction [3,4]. Various physicochemical and biological methods such as electrocoagulation, ozonation, photocatalysis, membrane filtration, biosorption, and adsorption have been employed for the treatment of dye containing wastewater [5,6]. Among these technologies, the adsorption process, which involves phase transfer of dye molecules onto adsorbent leaving behind the clear effluent, is considered to be a promising technology. Adsorption is considered to be a cheap method for dye removal. It is carried out by using low-cost adsorbents such as wood, charcoal, and biosorbents [5,7,8]. Adsorption, by activated carbon, has the most extensive application in this regard due to the high mesoporous nature, surface area, and high adsorption capacity. Yet, it has limited use due to high operational costs and nonregenerable features. For this reason, there is a need to develop economic alternative materials for waste treatment. Many biosorbents such as *Azadirachta indica* [3], raw pine [5], *Aspergillus niger* [7], Coir pith carbon [9], rice husk ash [10], jute stick powder [11], cattail root [12], *Trametes versicolor* [13], and jujuba seeds [14] have been used for removal and recovery of CR from aqueous solution.

*Saccharum bengalense* (SB), locally known as “Kana” or “Sarkanda” (Urdu/Pakistan) and Munja (Hindi/India) is a fast-growing annual herbage and is distributed from north and north west India to Pakistan and Afghanistan. It belongs to the Poaceae family as per ICBN and has a tall caespitose perennial with culms up to 4 m high. The leaf blades can measure up to 90 cm long, 3–10 mm wide, flat or markedly channeled, with the mid-rib occupying the greater part of the width, glaucous [15]. A valuable “pulp” material can be prepared from the upper leaf-sheaths of the flowering culm of the stem of SB plant, which can produce large quantities of biomass offering a good basis for the selection of SB as a cost-effective biosorbent. To the best of our knowledge, no investigations have been reported to explore the biosorption characteristics of this plant for the removal of toxic substances.

In the present study, biomass derived from the pulp of SB was used as an adsorbent material for the removal of toxic CR dye. The effect of various operating variables, viz. adsorbent dosage, contact time, pH, and temperature on the removal of CR dye has been studied. The efficiency of the process has been studied in terms of biosorption kinetics. Equilibrium parameters have been evaluated by applying Langmuir, Freundlich, and D–R isotherm models to the sorption data. Spontaneity and feasibility of the process has been studied by evaluating thermodynamic parameters such as free energy change ( $\Delta G^\circ$ ), enthalpy

change ( $\Delta H^\circ$ ), and entropy change ( $\Delta S^\circ$ ) at various temperatures.

## 2. Materials and methods

### 2.1. Adsorbate—CR

CR, an anionic disazo direct dye, was obtained from Sigma Aldrich (UK) of 99.99% purity. CR has molecular formula:  $C_{32}H_{22}N_6Na_2O_6S_2$  with molecular weight of 696.66 g/mol. It is the sodium salt of 3,3'-([1,1'-biphenyl]-4,4'-diyl) bis (4-aminonaphthalene-1-sulfonic acid). A stock solution of 1,000 mg/L was prepared by dissolving the appropriate amount (1.0 g) of CR in 1 L of deionized water. The chemical structure of CR dye is shown in Fig. 1(a).

### 2.2. Biosorbent—SB

SB was collected from the banks of the river Satluj in Bahawalpur, Pakistan. The SB samples were washed to remove any dust, or other foreign particles, and dried under shade after which the samples were milled in a standard laboratory knife mill to pass through a 60-mesh screen. The 100–250  $\mu\text{m}$  particles were collected and washed with deionized water.

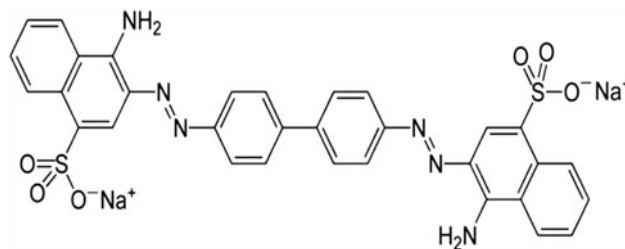


Fig. 1(a). Structure of CR (Na—Salt).

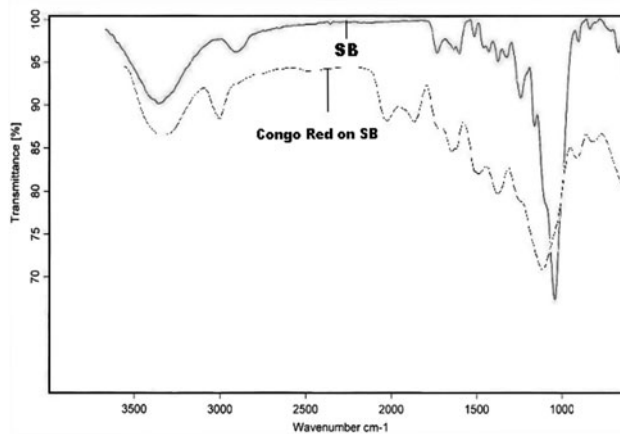


Fig. 1(b). FTIR spectra of SB and CR loaded on SB.

Finally the samples were oven dried (333 K) to constant mass and stored in air tight plastic bottles.

### 2.3. Batch biosorption studies

A series of experiments were carried out to study the effects of optimization parameters (biosorbent dose, pH, contact time, and temperature) of biosorption for the dye solution (40 mg/L, 50 mL) onto SB. Stock solutions (1,000 mg/L) of CR dye were prepared in deionized and double distilled water, then further diluted to obtain the desired concentration of dye. The pH adjustments were made with a digital pH meter (Jenway Model-3320) using 0.1 M HCl and 0.1 M NaOH. CR dye concentration for each experiment was found using a UV-vis Spectrophotometer (Labomed Model-UVD3500, USA) at 497 nm. The residual CR dye concentration in the reaction mixture was analyzed by centrifuging the reaction mixture. All experiments were carried out in triplicate and all values mentioned in the results are an average of three observations.

The percentage removal efficiency of adsorbent and uptake capacity ( $q_e$ ) were calculated as follows,

$$\% \text{ Removal (R\%)} = \frac{C_0 - C_e}{C_0} \times 100 \quad (1)$$

$$\text{Uptake capacity } q_e (\text{mg/g}) = [C_0 - C_e] \times \frac{V}{m} \quad (2)$$

where  $C_0$  (mg/L) and  $C_e$  (mg/L) are the initial and equilibrium dye concentrations, respectively.  $V$  is the volume of the solution in liters and  $m$  is the mass of the biosorbent in grams.

### 2.4. Adsorption kinetics

Biosorption kinetics explains the relationship of dye uptake rate of the biosorption and the adsorption time. In order to investigate the adsorption kinetics, different kinetic models including pseudo-first-order, pseudo-second-order, intra-particle diffusion, and Bangham's models were applied to the sorption data.

#### 2.4.1. Pseudo-first-order

The pseudo-first-order model is expressed by the following equation:

$$\frac{dq_t}{dt} = k_1(q_e - q_t) \quad (3)$$

where  $q_t$  and  $q_e$  (mg/g) are the amount of metal ions adsorbed on per unit weight of adsorbent at time  $t$  and equilibrium, respectively;  $k_1$  ( $\text{min}^{-1}$ ) is the pseudo-first-order rate constant of the sorption process.

By applying the boundary conditions  $t=0$  to  $t=t$  and  $q_t=0$  to  $q_t=q_t$  and integrating, the following equation is obtained:

$$\ln(q_e - q_t) = \ln q_e - k_1 t \quad (4)$$

$q_e$  and the rate constant ( $k_1$ ) can be evaluated from the intercept and the slope of linear plots of  $\ln(q_e - q_t)$  vs.  $t$  [16].

#### 2.4.2. Pseudo-second-order model

This model is based on the assumption that adsorption rate is proportional to the square of the number of unoccupied sites.

$$\frac{dq_t}{dt} = k_2(q_e - q_t)^2 \quad (5)$$

where  $k_2$  ( $\text{gm g}^{-1} \text{min}^{-1}$ ) is the rate constant of the pseudo-second-order.

The most commonly used linearized form of pseudo-second-order is given as [17]:

$$\frac{t}{q_t} = \frac{1}{k_2 q_e^2} + t/q_e \quad (6)$$

The constant  $k_2$  is used to calculate the initial sorption rate  $h$ , at  $t \rightarrow 0$ , as follows:

$$h = k_2 q_e^2$$

Thus, the rate constant  $k_2$ , initial adsorption rate ( $h$ ) and predicted  $q_e$  can be calculated from the plot of  $t/q$  vs. time ( $t$ ) [18].

#### 2.4.3. The intra-particle diffusion equation

The intra-particle diffusion equation can be written as follows[19]:

$$q_t = K_{id} \sqrt{Ot} + C \quad (7)$$

where  $k_{id}$  is the intra-particle diffusion rate constant ( $\text{mg g}^{-1} \text{min}^{-1/2}$ ) and  $C$  is the intercept.

By using this model, the plot of  $q_t$  ( $\text{mg g}^{-1}$ ) vs. the square root of time ( $t^{1/2}$ ) should be linear if the intra-particle diffusion is involved in the adsorption

process and, if these lines pass through the origin, then the intra-particle diffusion is the rate-controlling step [20].

#### 2.4.4. Bangham's equation

Bangham's equation has been applied to determine whether pore diffusion is the only rate-controlling step in the adsorption system [21]. Bangham's equation can be represented as

$$\log\left(\frac{C_0}{C_0 - q_t \times m}\right) = \log\left(\frac{k_B \times m}{2.303 \times v}\right) + [\alpha] \ln(t) \quad (8)$$

where  $C_0$  is the initial concentration of adsorbate in solution (mg/L),  $q_t$  (mg/g) is the amount of adsorbate retained at time  $t$ ,  $\alpha$  ( $<1$ ) and  $k_B$  are constants,  $V$  is the volume of solution (L), and  $m$  is the mass (g) of adsorbent per liter of solution.

### 3. Results and discussion

#### 3.1. Characterization of SB

Biomass SB was characterized by elemental analysis, BET surface area, and FTIR analysis. Elemental analysis was accomplished by *Perkin Elmer 2400 Series II CHNS/O Elemental Analyzer using sulfanilamide as the standard*. A potassium bromide disc method was used to scan the FTIR spectra in the range 4,000–450  $\text{cm}^{-1}$  using FTIR spectrophotometer (Tensor 27, Bruker Germany). BET surface area and single point surface area of SB was determined from the  $\text{N}_2$  adsorption isotherm at 77K in the range of relative pressure  $10^{-6}$ –1.0 with a surface area and pore size

analyzer (Autosorb 1, Quantachrome Instruments.). Before measurement, the sample was degassed at 300 °C for 2 h. The results for elemental analysis, BET surface area, and FTIR are given in Table 1.

From the comparison of FTIR spectra of SB and CR dye-loaded SB (CR-SB), it was found that CR dye mostly attached with the oxygen containing functional groups. Thus, the functional groups such as OH, COOH, and  $\text{OCH}_3$  play an important role in the biosorptive removal of CR dye from aqueous solutions.

It can be confirmed from Fig. 1(b) that there were clear shifts in the positions of the bands obtained from oxygen containing functional groups i.e. from 3,359.83 to 3,342.64  $\text{cm}^{-1}$  (O–H), 1,039.44 to 1,051.20  $\text{cm}^{-1}$  (–O–C), and from 1,730.99 to 1,724.36  $\text{cm}^{-1}$  (–COOH) [18].

#### 3.2. The pH of zero of point charge

The  $\text{pH}_{\text{ZPC}}$  was determined for SB in terms of the difference in pH solution, before and after soaking, with potassium nitrate [22]. To a series of 100 mL conical flasks, 45 mL of known concentration of 0.01 M  $\text{KNO}_3$  solution was transferred. The pH values of the solutions were adjusted from pH 2–10 by addition of 0.1 M HCl or NaOH. The total volume of the solution in each flask was made up to 50 mL by adding  $\text{KNO}_3$  solution of the same strength. The pH of the solution was accurately noted, and 0.1 g of SB powder was added to the flask. The flasks were then capped securely. The suspensions were then manually shaken and allowed to equilibrate for 24 h with intermittent manual shaking. The pH values of the supernatant liquids were noted. The difference between the initial and final pH values was plotted against the pH (figure not shown). The point of intersection of the

Table 1  
FTIR, physical, and chemical analysis of SB

Elemental analysis (%wt.)		Physical analysis	
C	41.2	BET surface area ( $\text{m}^2/\text{g}$ )	9.43
H	4.2	Single point surface area ( $\text{m}^2/\text{g}$ )	5.78
N	0.9	Porosity	0.043
Moisture (%)	3.1 ± 0.1		
Ashes (%)	1.1 ± 0.1		
pHz	6.26		
FTIR (wave number)			
SB	CR-SB	Assignment	
3,356.93	3,342.64	OH stretching	
2,913.29	2,891.30	Stretching vibration of the C–H	
1,730.99	1,724.36	C–O, C–C stretching	
1,425.49	1440.83	C–H bending	
1,039.44	1,051.20	C–O–C stretching	

resulting curve, at which  $\Delta\text{pH}=0$ , gave the  $\text{pH}_{\text{PZC}}$  value. Untreated SB has a  $\text{pH}_{\text{ZPC}}$  value of 6.26 [23,24].

### 3.3. Effect of adsorbent dosage

The effect of adsorbent dosage on adsorption of CR dye was studied using different dosage in the range, 0.1–1.0 g/50 mL (Fig. 2(a)). The dye concentration in each case was recorded (40 mg/L, 50 mL). Results showed that the adsorption efficiency is highly dependent on quantity of adsorbent added. Maximum removal of dye was 90%. This was expected, as with increasing concentration of adsorbent, more active sites became available for CR dye uptake. Similar biosorbent dose behavior for dye adsorption onto various adsorbents was reviewed [2]. The decrease in efficiency at the higher adsorbent concentrations could be explained as a consequence of a partial aggregation of adsorbent, which results in a decrease in effective surface area for dye uptake [25]. Therefore, the optimum dosage was selected as 0.5 g/50 mL.

### 3.4. Effect of pH

The pH of the dye solution plays an important role on the biosorption capacity, surface charge of the biosorbent, degree of ionization of the material present in the solution, and the dissociation of functional groups on the active sites of the biosorbent. CR is a dipolar molecule ( $\text{H}_3\text{N}^+-\text{R}-\text{SO}_3^-$ ) at low pH.

SB contains a variety of functional groups including  $-\text{OH}$  and  $-\text{COOH}$  which could also be affected by the pH of solutions. The biosorption of CR onto SB is highly pH dependent. It is reported that the molecular form of CR in solution could change significantly at a

low pH of 1–4 and at a high pH of 10–12 [14]. In pH studies, it was observed that when pH was 2, the dye solution changed its color from red to dark blue with fine particles in suspension in the solution which resulted in high removal efficiency by the filter. At higher pH values of 10–12, the degree of red color was different from the original red. After adjustment of pH to 7.5, all solutions had the same degree of red, which indicated that the adjustment of pH to 7.5 before measurement was necessary. Similar behavior of CR dye solution was reported earlier [7].

With the increasing pH values, the adsorption of CR dye on SB biomass tends to decrease, because the repulsion between the colored anions of CR dye and the negatively charged SB increased causing a decrease in biosorption capacity. The presence of excess  $\text{OH}^-$  ions also lowers the adsorption at alkaline pH due to the destabilizing anionic dye and competition with the dye anions for the adsorption sites [5]. In order to investigate the effect of pH on the CR removal by SB, experiments were carried out over a pH range of 1–10.0 at CR concentration 40 mg/L, SB dosage 0.5 g/50 mL, and temperature 40 °C. The maximum removal of CR was achieved at pH 2 as shown in Fig. 2(b). The maximum removal efficiency of CR dye for SB was 89.3%.

### 3.5. Adsorption isotherms

Isotherm studies provide information about the capacity of the adsorbent material  $q_e$  (mg/g) or the amount required to remove a unit mass of pollutant toxic dyes from water. The adsorption data have been subjected to Langmuir, Freundlich, and

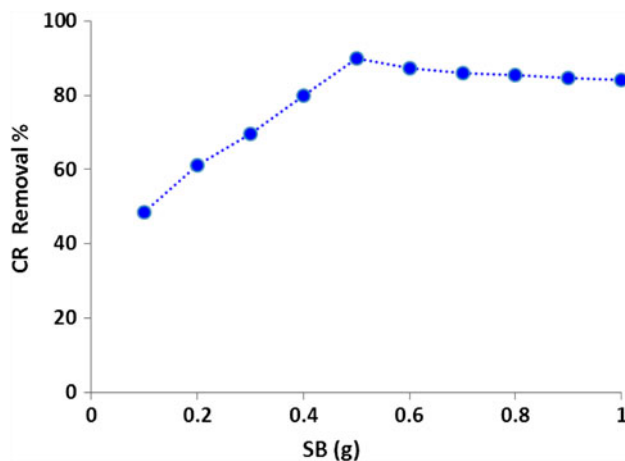


Fig. 2(a). Effect of adsorbent dose at 50 °C; size of SB <125  $\mu\text{m}$ ; speed of agitation 125 rpm and pH 2.0.

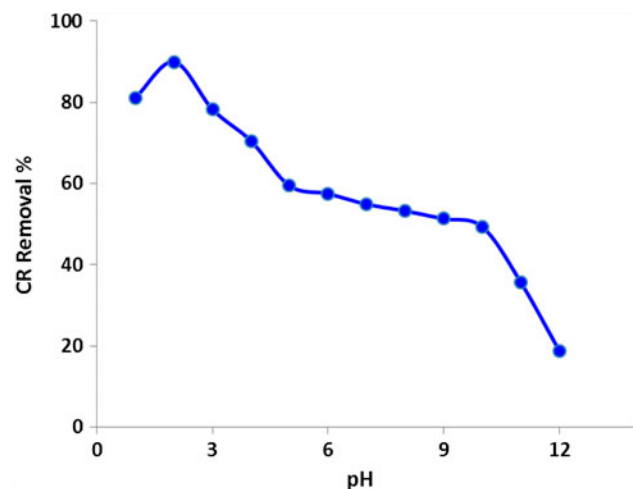


Fig. 2(b). Effect of pH for sorption of CR dye on SB at 50 °C; size of SB <125  $\mu\text{m}$ ; speed of agitation 125 rpm and SB dose 0.5 g/50 mL.

Dubinin–Radushkevich (D–R) isotherm models to predict the mechanism of adsorption.

### 3.5.1. Langmuir adsorption isotherm

The Langmuir model assumes uniform energies of adsorption onto the surface and no transmigration of adsorbate in the plane of the surface. Langmuir's isotherm has been used by various workers for the sorption of a variety of compounds and the simplest linear form of this isotherm is given by the following equation [26,27].

$$\frac{1}{q_e} = \left[ \frac{1}{K_L q_{\max}} \times \frac{1}{C_e} \right] + \frac{1}{q_{\max}} \quad (9)$$

where  $q_e$  is the equilibrium dye concentration on the adsorbent (mg/g);  $C_e$ , the equilibrium concentration in solution (mg/L);  $q_{\max}$ , the monolayer adsorption capacity of the adsorbent (mg/g);  $K_L$ , the Langmuir constant (L/mg) related to the free energy of adsorption.

Hence, a linear plot of  $1/q_e$  vs.  $1/C_e$  for the Langmuir adsorption isotherm gives a straight line of slope  $1/(q_{\max} K_L)$  and intercept  $1/q_{\max}$ .

### 3.5.2. Separation factor

The Langmuir adsorption isotherm can be classified by a dimensionless constant separation factor ( $R_L$ ), given as [8].

$$R_L = \frac{1}{1 + K_L C_0} \quad (10)$$

where  $C_0$  (mg/L) is the initial dye concentration and  $K_L$  (L/mg) is the Langmuir constant related to the energy of adsorption. The value of  $R_L$  indicates the shape of the isotherms to be [28]:

- (a) Unfavorable:  $R_L > 1$
- (b) linear:  $R_L = 1$
- (c) favorable ( $0 < R_L < 1$ )
- (d) Irreversible  $R_L = 0$

### 3.5.3. Freundlich isotherm

The adsorption data of CR was also applied to the Freundlich model. The logarithmic form of the Freundlich model [29] is given by the following equation:

$$\ln q_e = \ln K_F + \frac{1}{n} \ln C_e \quad (11)$$

where  $q_e$  is the amount adsorbed (mg/g),  $C_e$  is the equilibrium concentration of the adsorbate (mg/L), and  $K_F$  and  $n$  are the Freundlich constants related to adsorption capacity and adsorption intensity, respectively. Freundlich parameters,  $n$  and  $K_F$ , are evaluated from linear plots of  $\ln q_e$  against  $\ln C_e$ .

### 3.5.4. D–R Model

The D–R isotherm model is more general than the Langmuir isotherm model due to the fact that it does not assume a homogeneous surface or constant adsorption potential. It determines the mean free energy of adsorption and helps distinguish between physical and chemical adsorption. The linear equation of the D–R isotherm [26] is

$$\ln q_e = \ln q_{\max} - \beta \varepsilon^2 \quad (12)$$

where  $\beta$  ( $\text{mol}^2/\text{J}^2$ ) is a constant connected with the mean free energy of adsorption per mole of the adsorbate and  $\varepsilon$  (J/mol) is the Polanyi potential which is given as:

$$\varepsilon = RT \ln \left( 1 + \frac{1}{C_e} \right) \quad (13)$$

where  $R$  (J/molK) is the gas constant and  $T$  (K) is the absolute temperature. Hence, by plotting  $\ln q_e$  vs.  $\varepsilon^2$ , it is possible to determine the value of  $q_m$  from the intercept and the value of  $\beta$  from the slope. The values of D–R parameters determined from Fig. 2(c) are given in Table 2.

The linearized Langmuir and Freundlich adsorption isotherms of CR dye on SB were presented in Fig. 3(a) and (b). The higher correlation coefficients value for Langmuir models indicated that this model is very suitable for describing the adsorption equilibrium of CR dye. The  $q_{\max}$  value for the Langmuir isotherm i.e. 125 mg/g, indicates the high adsorption capacity of SB towards CR adsorption. The  $R^2$  (determination coefficient) value, i.e. 0.958 close to unity, indicates that the Langmuir isotherm fits well to explain CR adsorption on SB. This was also confirmed by the  $R_L$  value. From Table 2, it was established that the value of  $R_L$  was in the range 0–1, validating the favorable uptake of the CR dye on SB.

From Table 2, the  $R^2$  value (0.964) for the Freundlich isotherm was found to be approaching near to one, indicating that the equilibrium sorption data

Table 2

Equilibrium isotherm parameters of biosorption of CR dye on SB at 50 °C and different initial CR concentrations. Conditions: size of SB <125 μm; pH of CR solution 2.0; dose of SB 0.5 g/50 mL; speed of agitation 125

Adsorption isotherm Linear form	Constant parameters			
	$q_{\max}$	$K_L$	$R^2$	$R_L$
<i>Langmuir isotherm</i> $\frac{1}{q_e} = \left[ \frac{1}{K_L q_{\max}} \times \frac{1}{C_e} \right] + \frac{1}{q_{\max}}$	125	0.00064	0.958	0.997
<i>Freundlich isotherm</i> $\ln q_e = \ln K_F + \left( \frac{1}{n} \right) \ln C_e$	$K_F$ 0.069	$n$ 0.931	$R^2$ 0.964	
<i>(D–R) isotherm</i> $\ln q_e = \ln q_{\max} - \beta \varepsilon^2$	$\beta$ $-3 \times 10^{-06}$	$q_m$ 1.23	$R^2$ 0.711	$E_s$ (kJmol <sup>-1</sup> ) 0.408

followed this isotherm. The “ $n$ ” value gives an idea whether the process is favorable or unfavorable under the studied conditions. The value of “ $n$ ” was 0.993 indicating that the adsorption onto the heterogeneous system is favorable. From Fig. 3(c), D–R parameters were calculated and presented in Table 2. The  $R^2$  value was 0.711, indicating that the biosorption of CR onto SB did not follow the D–R isotherm. The mean free energy of adsorption ( $E_s$ ) was found to be 0.408 kJ/mol, indicating adsorption was physical in nature. Since the D–R model is not being followed by this biosorption system, the  $E_s$  value provides only an assessment of the nature of the processes.

### 3.6. Effect of contact time: adsorption kinetics

The effect of the contact time on dye adsorption was studied by varying the time of contact from 10 to 70 min, at pH 2, and SB dosage of 0.5 g/50 mL. The dye removal efficiency (R%) increased from 44.48 to 94.14%. Increase in removal efficiency with an increase

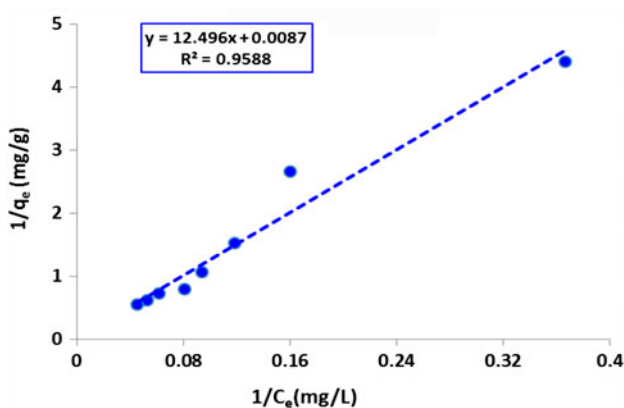


Fig. 3(a). Langmuir adsorption isotherm for sorption of CR dye on SB at 50 °C and different initial CR concentrations. Conditions: size of SB <125 μm; pH of CR solution 2.0; dose of SB 0.5 g/50 mL; speed of agitation 125 rpm.

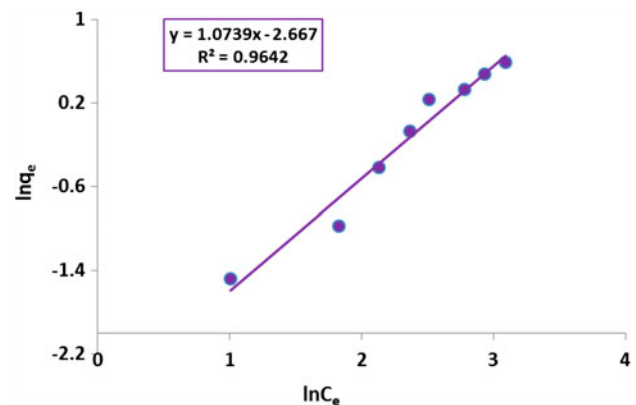


Fig. 3(b). Freundlich adsorption isotherm for sorption of CR dye on SB at 50 °C and different initial CR concentrations. Conditions: size of SB <125 μm; pH of CR solution 2.0; dose of SB 0.5 g/50 mL; speed of agitation 125 rpm.

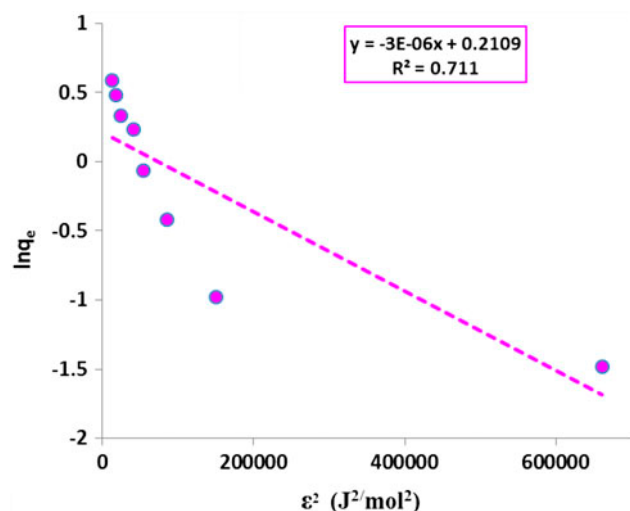


Fig. 3(c). D–R adsorption isotherm for sorption of CR dye on SB at 50 °C and different initial CR concentrations. Conditions: size of SB <125 μm; pH of CR solution 2.0; dose of SB 0.5 g/50 mL; speed of agitation 125 rpm.

in time of contact is due to the fact that more time becomes available for CR dye molecules to adsorb onto SB. Initial removal occurs immediately as soon as the dye and biomass come into contact. After some time, the number of active sites decrease and so the dye molecules need more time to find more active sites for binding [28]. Therefore, further adsorption experiments were carried out for CR dye onto SB at 50 min by which maximum dye was removed (94.14%).

The pseudo-first-order, pseudo-second-order, and intra-particle diffusion kinetic models were applied to evaluate the kinetic parameters from sorption data.

The plots of  $\ln(q_e - q_t)$  vs.  $t$  for the pseudo-first-order model are shown in Fig. 4(a) and the  $R^2$  value obtained was 0.621 indicating that the adsorption of CR dye onto SB biomass did not follow the pseudo-first-order kinetic model [6].

The linear plots of  $t/qt$  vs.  $t$  for the pseudo-second-order model for the biosorption CR dye onto SB are shown in Fig. 4(b). For pseudo-second-order, the  $R^2$  value was near to unity (0.974). In addition, the calculated  $q_e$  value (3.7 mg/g) was comparable to the experimental  $q_e$  (3.69 mg/g) value. Hence, it can be concluded that biosorption of CR by SB followed the pseudo-second-order kinetic model. Values of different parameters for pseudo-second-order model at different CR dye concentrations from 10 to 40 mg/L were calculated from Fig. 4(b) and are given in Table 3(a).

The intra-particle diffusion model was applied to find the rate-determining step. The linear plots of  $q_t$  vs.  $t^{1/2}$  for the intra-particle diffusion model are shown in Fig. 4(c). This plot shows the dual nature of the curves owing to the varying extent of biosorption in the initial and final stages of the process for CR biosorption on SB. This phenomenon indicated that more

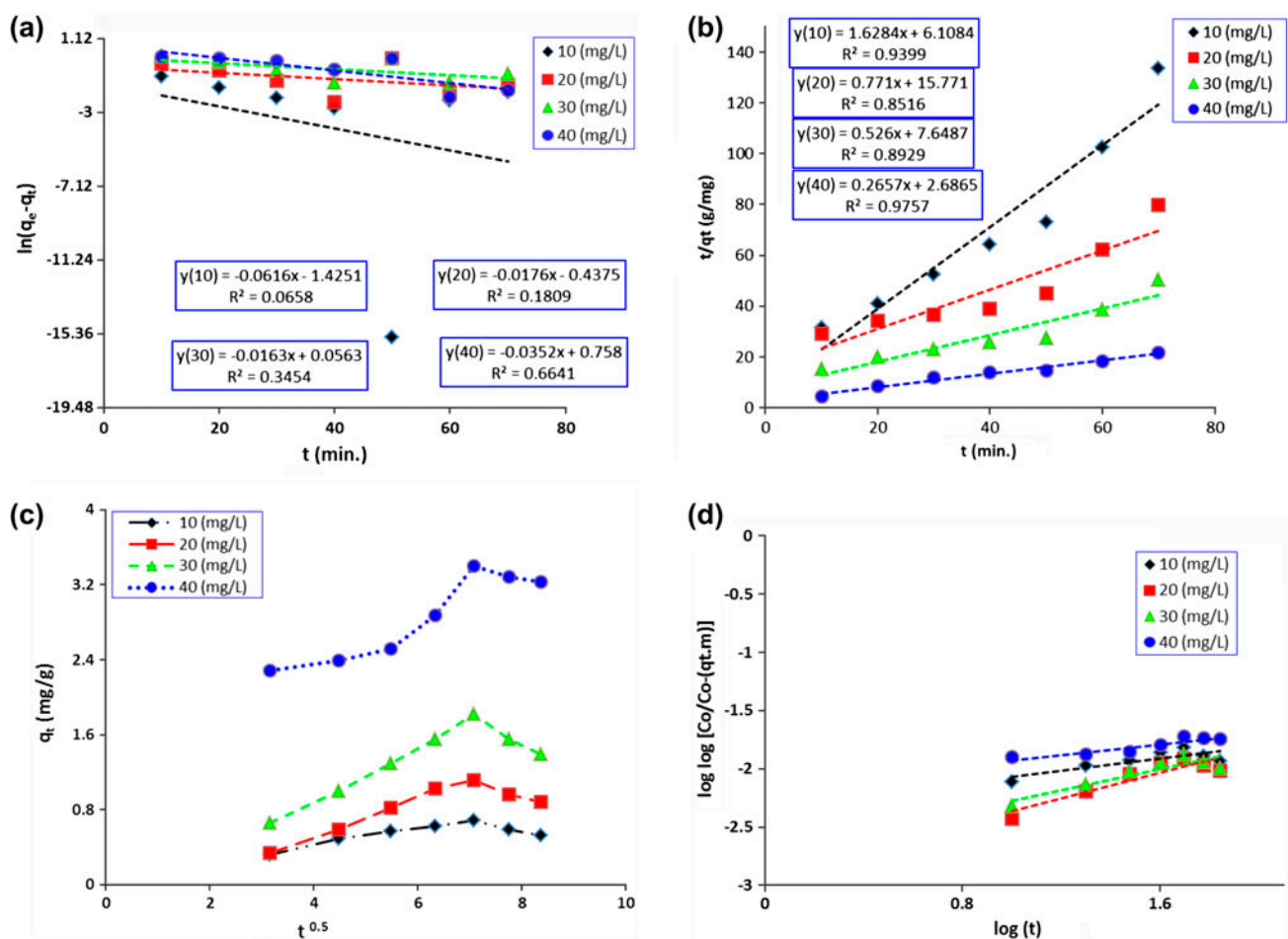


Fig. 4. (a) Pseudo-first-order kinetics, (b) Pseudo-second-order kinetics, (c) Intra-particle diffusion kinetic model, and (d) Bangham kinetic model for sorption of CR on SB at 50 °C and different initial CR concentrations. Conditions: size of SB <125  $\mu$ m; pH of CR solution 2.0; dose of SB 0.5 g/50 mL; speed of agitation 125 rpm. The kinetic parameters for the adsorption of CR dye onto SB are summarized in Tables 3a and 3b.

Table 3

Pseudo-first-order and pseudo-second-order rate constants at 50 °C and different initial CR concentrations. Conditions: size of SB < 125 µm; pH of CR solution 2.0; dose of SB 0.5 g/50 mL; speed of agitation 125 rpm

C <sub>0</sub> (mg/L)	q <sub>e exp</sub> (mg/g)	Pseudo-first-order			Pseudo-second-order			Bangham kinetic model		
		k <sub>1</sub> (min <sup>-1</sup> )	q <sub>e cal</sub> (mg/g)	R <sup>2</sup>	k <sub>2</sub> (g mg <sup>-1</sup> min <sup>-1</sup> )	q <sub>e cal</sub> (mg/g)	R <sup>2</sup>	α	k <sub>B</sub>	R <sup>2</sup>
10	0.6	0.062	0.241	0.065	0.434	0.6	0.940	0.255	0.00109	0.663
20	1.1	0.018	0.646	0.180	0.038	1.3	0.852	0.552	0.00002	0.826
30	1.8	0.016	0.945	0.345	0.036	1.9	0.893	0.457	0.00042	0.822
40	3.4	0.035	2.134	0.664	0.026	3.7	0.976	0.224	0.00163	0.843

Table 4

Intra-particle diffusion constants for different initial CR concentrations at 50 °C and different initial CR concentrations. Conditions: size of SB < 125 µm; pH of CR solution 2.0; dose of SB 0.5 g/50 mL; speed of agitation 125 rpm

Linear portion	Constants	Co = 10 mg/L	Co = 20 mg/L	Co = 30 mg/L	Co = 40 mg/L
First	K <sub>p1</sub> (mg g <sup>-1</sup> min <sup>0.5</sup> )	0.012	0.023	0.032	0.012
	C <sub>1</sub> (mg g <sup>-1</sup> )	2.160	0.105	0.349	2.164
	R <sup>2</sup>	0.995	0.999	0.998	0.995
Second	K <sub>p2</sub> (mg g <sup>-1</sup> min <sup>0.5</sup> )	0.044	0.015	0.026	0.044
	C <sub>2</sub> (mg g <sup>-1</sup> )	1.164	0.398	0.504	1.164
	R <sup>2</sup>	0.981	0.945	0.999	0.986
Third	K <sub>p3</sub> (mg g <sup>-1</sup> min <sup>0.5</sup> )	-0.008	-0.012	-0.021	-0.008
	C <sub>3</sub> (mg g <sup>-1</sup> )	3.810	1.678	2.865	3.813
	R <sup>2</sup>	0.953	0.977	0.978	0.953

than one type of diffusion process is involved in the biosorption. Since the curve is not linear, and does not pass through the origin, as intercept "C" is not zero, the boundary layer diffusion was found to be the rate-determining step for the biosorption of CR on SB [18]. The values of intra-particle diffusion model parameters were calculated from Fig. 4(c) and are given in Table 4.

Kinetic data can further be used to verify whether pore diffusion was the only rate-controlling step in the adsorption system using Bangham's equation. The correlation coefficient (R<sup>2</sup>) values obtained were 0.663, 0.826, 0.822, and 0.843 for 10, 20, 30, and 40 mg/L CR dye concentrations, respectively, indicating pore diffusion was not the only rate-limiting step and Bangham's expression did not conform to the experimental data. With increase in contact time, the effect of the diffusion process on the overall adsorption could be ignored [30]. The values of Bangham parameters were calculated from Fig. 4(d) and given in Table 3(a).

### 3.7. Effect of temperature: thermodynamics

Effect of temperature was studied in the range 293–323 K at pH 2.0, while the following conditions were kept constant: adsorbate concentration 40 mg/L

and adsorbent concentration 0.5 g/50 mL. An increase in temperature from 293 to 313 K indicated an increase in percentage adsorption removal (R%) from 56.92 to 93.42% exhibiting the endothermic nature of the adsorption process of CR on SB [31]. Therefore, 313 K was selected as the optimum temperature for maximum CR dye removal (93.42%) by SB.

Thermodynamic parameters such as standard Gibbs free energy ΔG°, enthalpy ΔH°, and entropy ΔS° were also calculated using Eqs. 14–16 and the results obtained are illustrated in Table 5 [32].

$$\Delta G^\circ = -RT \ln K_D \quad (14)$$

$$\ln K_D = C_s / C_e \quad (15)$$

$$\ln K_D = \frac{\Delta S}{R} - \frac{\Delta H}{RT} \quad (16)$$

where K<sub>D</sub> denotes the distribution coefficient for the adsorption, R (8.3143 J/mol K) is universal gas constant, T is absolute temperature in Kelvin, and C<sub>s</sub> (mg/L) is the equilibrium amount of dye adsorbed on the adsorbent per liter of the solution. The values of ΔG°, ΔH°, and ΔS° are evaluated from Fig. 5 and illustrated in Table 4.

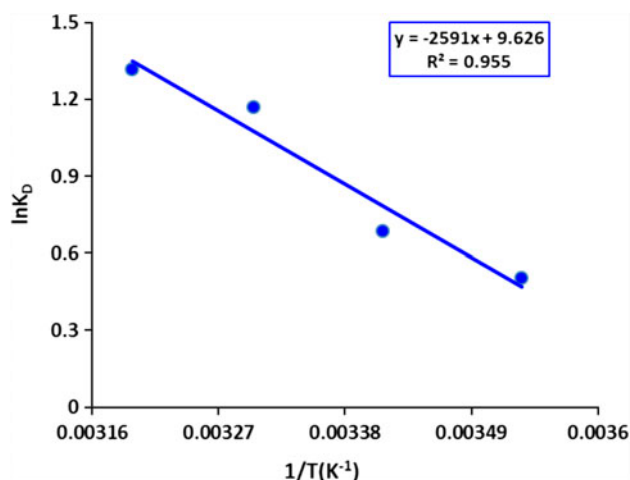


Fig. 5. Thermodynamics parameters for the sorption of CR on SB at different temperatures. Conditions: size of SB <125  $\mu\text{m}$ ; pH of CR solution 2.0; dose of SB 0.5 g/50 mL; speed of agitation 125 rpm.

Table 5  
Thermodynamics parameters for sorption of CR on SB at different temperatures; size of SB <125  $\mu\text{m}$ ; pH of CR solution 2.0; dose of SB 0.5 g/50 mL; speed of agitation 125 rpm

Temp (K)	$K_D$	$\Delta G^0$ (kJmol <sup>-1</sup> )	$\Delta S^0$ (kJmol <sup>-1</sup> K <sup>-1</sup> )	$\Delta H^0$ (kJmol <sup>-1</sup> )
283	1.655	-1,185.53	0.080	+21.54
293	1.990	-1,676.53		
303	3.219	-2,944.98		
313	3.738	-3,431.31		
323	6.333	-4,956.46		

The negative value of  $\Delta G^0$  over the studied temperature range indicates that the sorption of CR onto SB biomass is thermodynamically feasible and spontaneous. The increase in value of  $\Delta G^0$  with temperature further shows the increase in feasibility of sorption at the elevated temperatures for SB. The positive value of  $\Delta H^0$  shows the endothermic nature of the biosorption process. The positive value of  $\Delta S^0$  reflects the strong affinity of SB for Congo red [31].

**Cost estimation:** SB collected from the banks of the river Satluj in Bahawalpur, Pakistan was totally free of cost. After considering the charges for chemicals, electrical energy, and transport, the final cost of adsorbent material would be approximately \$62/tonne.

### 3.8. Comparison of adsorption capacity of SB with different adsorbents

SB has been compared with various biosorbents in terms of adsorption capacity (mg/g). Table 6 shows such a comparison.

Table 6  
Comparison of adsorption potential of various adsorbents for CR removal from aqueous solution

Adsorbent	$q_{\text{max}}$ (mg/g)	Reference
(1) Coir pith carbon	6.7	[9]
(2) Rice husk ash	7.04	[10]
(3) <i>Aspergillus niger</i>	14.16	[7]
(4) Raw pine	32.65	[5]
(5) Jute stick powder	35.7	[11]
(6) Cattail root	38.79	[12]
(7) <i>Azadirachta indica</i>	41.2	[3]
(8) <i>Trametes versicolor</i>	51.81	[13]
(9) Jujuba seeds	55.56	[14]
(10) SB	125.41	Present work

## 4. Conclusion

It can be concluded that SB is an effective and eco-friendly biosorbent for the removal of CR dye from aqueous solutions. The uptake of CR dye on SB is highly dependent on the chemical structure of the dye, pH, and the functional groups present in SB biomass. The biosorption kinetics can be determined by pseudo-second-order kinetics. The Langmuir model is found to provide the best fit to the experimental data with a maximum biosorption capacity of 125 mg/g. Thermodynamic studies show that adsorption of CR on SB is a feasible, spontaneous, and favorable process. SB has been compared with various biosorbents in terms of adsorption capacity (mg/g). It is easily observed that the adsorption capacity of SB is high as compared to a number of other adsorbents and it may be concluded that SB is an effective biosorbent for the removal of toxic CR dye from aqueous water.

## Acknowledgment

The authors wish to thank Mr. Manzar Islam (University of the Punjab, Lahore) for his supportive technical assistance and guidance.

## References

- [1] A. Bhatnagar, A.K. Jain, M.K. Mukul, Removal of congo red dye from water using carbon slurry waste, *Environ. Chem. Lett.* 2 (2005) 199–202.
- [2] M.A.M. Salleh, D.K. Mahmoud, W.A.W.A. Karim, A. Idris, Cationic and anionic dye adsorption by agricultural solid wastes: A comprehensive review, *Desalination* 280 (2011) 1–13.
- [3] K.G. Bhattacharyya, A. Sharma, *Azadirachta indica* leaf powder as an effective biosorbent for dyes: A case study with aqueous Congo red solutions, *J. Environ. Manage.* 71 (2004) 217–229.
- [4] F.A. Pavan, S.L.P. Dias, E.C. Lima, E.V. Benvenutti, Removal of congo red from aqueous solution by anilinepropylsilica xerogel, *Dyes Pigm.* 76 (2008) 64–69.

- [5] S. Dawood, T.K. Sen, Removal of anionic dye Congo red from aqueous solution by raw pine and acid-treated pine cone powder as adsorbent: Equilibrium, thermodynamic, kinetics, mechanism and process design, *Water Res.* 46 (2012) 1933–1946.
- [6] Y. Yang, G. Wang, B. Wang, Z. Li, X. Jia, Q. Zhou, Y. Zhao, Biosorption of acid black 172 and Congo red from aqueous solution by nonviable penicillium YW 01: Kinetic study, equilibrium isotherm and artificial neural network modeling, *Bioresour. Technol.* 102 (2011) 828–834.
- [7] Y. Fu, T. Viraraghavan, Removal of Congo red from an aqueous solution by fungus *Aspergillus niger*, *Adv. Environ. Res.* 7 (2002) 239–247.
- [8] A.E. Ofomaja, Y.-S. Ho, Equilibrium sorption of anionic dye from aqueous solution by palm kernel fibre as sorbent, *Dyes Pigm.* 74 (2007) 60–66.
- [9] C. Namasivayam, D. Kavitha, Removal of Congo red from water by adsorption onto activated carbon prepared from coir pith, an agricultural solid waste, *Dyes Pigm.* 54 (2002) 47–58.
- [10] A.K. Chowdhury, A.D. Sarkar, A. Bandyopadhyay, Rice husk ash as a low cost adsorbent for the removal of methylene blue and Congo red in aqueous phases, *Clean, Soil, Air, Water* 37 (2009) 581–591.
- [11] G.C. Panda, S.K. Das, A.K. Guha, Jute stick powder as a potential biomass for the removal of congo red and rhodamine B from their aqueous solution, *J. Hazard. Mater.* 164 (2009) 374–379.
- [12] Z. Hu, H. Chen, F. Ji, S. Yuan, Removal of Congo red from aqueous solution by cattail root, *J. Hazard. Mater.* 173 (2010) 292–297.
- [13] A.R. Binupriya, M. Sathishkumar, K. Swaminathan, C.S. Kuz, S.E. Yun, Comparative studies on removal of Congo red by native and modified mycelial pellets of *Trametes versicolor* in various reactor modes, *Bioresour Technol.* 99 (2008) 1080–1088.
- [14] M.C. Somasekhara Reddy, L. Sivaramakrishna, A. Varada Reddy, The use of an agricultural waste material, Jujuba seeds for the removal of anionic dye (Congo red) from aqueous medium, *J. Hazard. Mater.* 203–204 (2012) 118–127.
- [15] S.A. Tirmzi, F.H. Watoo, M.H.S. Watoo, S. Kanwal, J. Iqbal, Inorganic nutrients of *Saccharum bengalense*, *J. Chem. Soc. Pak.* 27 (2005) 186–189.
- [16] U. Farooq, M.A. Khan, M. Athar, M. Sakina, M. Ahmad, Environmentally Benign Urea-modified *Triticum aestivum* Biomass for Lead (II) Elimination from Aqueous Solutions, *Clean, Soil, Air, Water* 38 (2010) 49–56.
- [17] Y.S. Ho, G. McKay, Pseudo-second order model for sorption processes, *Process Biochem.* 34 (1999) 451–465.
- [18] U. Farooq, M.A. Khan, M. Athar, J.A. Kozinski, Effect of modification of environmentally friendly biosorbent wheat (*Triticum aestivum*) on the biosorptive removal of cadmium(II) ions from aqueous solution, *Chem. Eng. J.* 171 (2011) 400–410.
- [19] W.J. Weber, Jr., J.C. Morriss, Kinetics of adsorption on carbon from solution, *J. Sanitary Eng. Div. Am. Soc. Civ. Eng.* 89 (1963) 31–60.
- [20] R.H.W. Zou, Z. Chen, Z. Jinghua, J. Shi, Kinetic study of adsorption of Cu(II) and Cd(II) from aqueous solutions using manganese oxide coated zeolite in batch mode, *Colloids Surf. A* 279 (2006) 238–246.
- [21] V.S. Mane, I. Deo Mall, V. Chandra Srivastava, Kinetic and equilibrium isotherm studies for the adsorptive removal of brilliant green dye from aqueous solution by rice husk ash, *J. Environ. Manage.* 84 (2007) 390–400.
- [22] V.C. Srivastava, I.D. Mall, I.M. Mishra, Characterization of mesoporous rice husk ash (RHA) and adsorption kinetics of metal ions from aqueous solution onto RHA, *J. Hazard. Mater.* 134 (2006) 257–267.
- [23] E.I. Unuabonah, K.O. Adebowale, F.A. Dawodu, Equilibrium, Kinetic and sorber design studies on the adsorption of aniline blue dye by sodium tetraborate-modified Kaolinite clay adsorbent, *J. Hazard. Mater.* 157 (2008) 397–409.
- [24] A.E. Ofomaja, E.B. Naidoo, S.J. Modise, Removal of copper(II) from aqueous solution by pine and base modified pine cone powder as biosorbent, *J. Hazard. Mater.* 168 (2009) 909–917.
- [25] V. Vadivelan, K.V. Kumar, Equilibrium, kinetics, mechanism, and process design for the sorption of methylene blue onto rice husk, *J. Colloid Interface Sci.* 286 (2005) 90–100.
- [26] B. Hameed, I. Tan, A. Ahmad, Adsorption isotherm, kinetic modeling and mechanism of 2, 4, 6-trichlorophenol on coconut husk-based activated carbon, *Chem. Eng. J.* 144 (2008) 235–244.
- [27] I. Langmuir, The constitution and fundamental properties of solids and liquids, *J. Am. Chem. Soc.* 38 (1916) 2221–2295.
- [28] E. Bulut, M. Özacar, İ.A. Şengil, Equilibrium and kinetic data and process design for adsorption of Congo Red onto bentonite, *J. Hazard. Mater.* 154 (2008) 613–622.
- [29] H.M.F. Freundlich, Über die adsorption in lösungen (Over the adsorption in solution), *Z. Phys. Chem.* 57 (1906) 385–470.
- [30] T.K. Naiya, A.K. Bhattacharya, S. Mandal, S.K. Das, The sorption of lead(II) ions on rice husk ash, *J. Hazard. Mater.* 163 (2009) 1254–1264.
- [31] F. Çolak, N. Atar, A. Olgun, Biosorption of acidic dyes from aqueous solution by *Paenibacillus macerans*: Kinetic, thermodynamic and equilibrium studies, *Chem. Eng. J.* 150 (2009) 122–130.
- [32] O.S. Lawal, A.R. Sanni, I.A. Ajayi, O.O. Rabi, Equilibrium, thermodynamic and kinetic studies for the biosorption of aqueous lead(II) ions onto the seed husk of *Calophyllum inophyllum*, *J. Hazard. Mater.* 177 (2010) 829–835.